Published in final edited form as:
Diabetes. 2008 January ; 57(1): 199–208. doi:10.2337/db07-0830.

Nonobese Diabetic (NOD) Mice Congenic for a Targeted Deletion of 12/15-Lipoxygenase Are Protected From Autoimmune Diabetes

Marcia McDuffie, **Nelly A. Maybee**, **Susanna R. Keller**, **Brian K. Stevens**, **James C. Garmey**, **Margaret A. Morris**, **Elizabeth Kropf**, **Claudia Rival**, **Kaiwen Ma**, **Jeffrey D. Carter**, **Sarah A. Tersey**, **Craig S. Nunemaker**, and **Jerry L. Nadler**
University of Virginia, Charlottesville, Virginia.

Abstract

OBJECTIVE—12/15-lipoxygenase (12/15-LO), one of a family of fatty acid oxidoreductase enzymes, reacts with polyenoic fatty acids to produce proinflammatory lipids. 12/15-LO is expressed in macrophages and pancreatic β-cells. It enhances interleukin 12 production by macrophages, and several of its products induce apoptosis of β-cells at nanomolar concentrations in vitro. We had previously demonstrated a role for 12/15-LO in β-cell damage in the streptozotocin model of diabetes. Since the gene encoding 12/15-LO (gene designation *Alox15*) lies within the *Idd4* diabetes susceptibility interval in NOD mice, we hypothesized that 12/15-LO is also a key regulator of diabetes susceptibility in the NOD mouse.

RESEARCH DESIGN AND METHODS—We developed NOD mice carrying an inactivated 12/15-LO locus (NOD-*Alox15*^{null}) using a “speed congenic” protocol, and the mice were monitored for development of insulitis and diabetes.

RESULTS—NOD mice deficient in 12/15-LO develop diabetes at a markedly reduced rate compared with NOD mice (2.5 vs. >60% in females by 30 weeks). Nondiabetic female NOD-*Alox15*^{null} mice demonstrate improved glucose tolerance, as well as significantly reduced severity of insulitis and improved β-cell mass, when compared with age-matched nondiabetic NOD females. Disease resistance is associated with decreased numbers of islet-infiltrating activated macrophages at 4 weeks of age in NOD-*Alox15*^{null} mice, preceding the development of insulitis. Subsequently, islet-associated infiltrates are characterized by decreased numbers of CD4^{+} T cells and increased Foxp3^{+} cells.

CONCLUSIONS—These results suggest an important role for 12/15-LO in conferring susceptibility to autoimmune diabetes in NOD mice through its effects on macrophage recruitment or activation.

The nonobese diabetic (NOD) mouse is a well-established animal model for type 1 diabetes (1). Genetic susceptibility in NOD mice has been mapped to more than 30 genetic regions, currently designated “insulin-dependent diabetes” (*Idd*) loci (2). Susceptibility determinants on mouse chromosome 11 were first recognized by linkage to the microsatellite *D11Nds1* after outcross of NOD to the C57BL/10 strain, with C57BL/10 alleles decreasing the

Address correspondence and reprint requests to Jerry L. Nadler, MD, University of Virginia, P.O. Box 801405, Charlottesville, VA 22908..

Part of the data were presented in abstract form at the 67th annual meeting of the American Diabetes Association, 22–26 June 2007, Chicago, Illinois.

severity of insulitis in young mice. Linkage to this region of chromosome 11, designated *Idd4* (3), was confirmed in a cross with the NOD-related NOR strain, which is a genetic mosaic of NOD with two nondiabetes-prone mouse strains: C57BL/6 and DBA/2. In this cross, DBA/2-derived alleles on chromosome 11 decreased the incidence of diabetes after administration of cyclophosphamide (4). Subsequently, congenic strains generated from crosses with C57L (5,6), C57BL/6 (7), and NOR (4,8) mice demonstrated that the initial mapping results were produced by a cluster of susceptibility loci, now designated *Idd4.1, Idd4.2,* and *Idd4.3* (also designated *Idd4a*). Functional polymorphisms of both *Stat5b* and *Il12b* (encoding the 40-kDa chain of interleukin [IL]-12, IL-12p40), located at the telomeric and centromeric ends of chromosome 11, respectively, have been identified in NOD mice (9–11) and may have contributed to evidence for linkage on chromosome 11 in the initial C57BL/10 cross. To date, however, no strong candidate genes for the *Idd4.1–4.3* loci, mapped to mid-chromosome, have been both identified and validated.

Based on its known functions and its genomic location, the 12/15-LO locus (*Alox15*) represents an excellent candidate for *Idd4.1*. Also known as "leukocyte 12-lipoxygenase," this enzyme catalyzes the oxygenation of polyenoic fatty acids (including arachidonic acid and linoleic acid) to form lipid inflammatory mediators, such as 12-hydroperoxyeicosatetraenoic acid (12-HPETE) and 13-(*S*)-hydroperoxy-9Z,11E-octadecedienoic acid (13-HPODE). Although 12/15-LO is expressed in other cell types, high levels of mRNA, protein, and enzyme activity are reported in macrophages and pancreatic β-cells from both mice and humans (12,13). 12-HPETE is toxic at physiological levels to β-cells, where it is also converted to a more stable metabolite 12-hydroxyeicosatetranoic acid (12-HETE) by glutathione peroxidase (14). 12-HETE is also directly toxic to β-cells and human islets, markedly decreasing insulin secretory function and increasing β-cell death (13). 12-HETE can be further metabolized to 12-HETrE, which acts as a proinflammatory agent and colocalizes with insulin in β-cells (15). 12-HETE can activate nuclear factor-kB, p38, stress-activated protein kinase JNK1/2, and p21-activated kinases—all possible mediators of cytokine-induced β-cell damage (13). It is reasonable to postulate, therefore, that the 12/15-LO activity may enhance the susceptibility of pancreatic β-cells to cytotoxic insults.

In addition to its activities in pancreatic β-cells, 12/15-LO regulates proinflammatory activity of myeloid cells, including macrophages. Macrophages are present in large numbers adjacent to the islets of young pre-diabetic NOD mice before the onset of substantial T-cell infiltration (16–21), and specific defects in macrophage development and function have been repeatedly demonstrated in NOD mice (6,22–30). Products of 12/15-LO activity stimulate expression of macrophage-derived cytokines, such as IL-12 (31), and these cytokines can upregulate 12/15-LO expression itself in a positive feedback loop, suggesting that it may also participate in β-cell destruction by enhancing the proinflammatory activity of islet-associated macrophages (32–34). A null mutation in mice ($Alox15^{tm1fun}$) reduces the atherogenic effects of loss of ApoE, presumably via demonstrated decreases in production of the arachidonic acid metabolites 12-HETE and 15-HETE in circulating macrophages (35). We have also demonstrated that mice homozygous for 12/15-LO mutation are markedly less susceptible to low-dose streptozotocin–induced diabetes than wild-type littermates (36). Thus, 12/15-LO may play an important role in enhancing tissue-specific inflammation in multiple settings in vivo.

To test the possibility that 12/15-LO may regulate disease susceptibility in the spontaneous diabetes of NOD mice, we generated NOD mice congenic for the $Alox15^{tm1fun}$ null mutation. We show that these mice are profoundly resistant to the development of diabetes. The decreased incidence of overt diabetes is associated with markedly diminished insulitis, as well as preservation of islet mass and function. Preceding these late events, we find that

loss of 12/15-LO activity prevents peri-islet accumulation of activated macrophages that are routinely seen in young NOD mice and leads to a significant decrease in $CD4^+$ T-cell infiltration into islets, along with increased numbers of $Foxp3^+$ cells, in mature animals. These findings suggest that 12/15-LO is a major regulator of initiation and progression of insulitis in the NOD mouse through its effects on the accumulation of macrophages in islet tissue and, further, that blockade of 12/15-LO activity may provide a novel strategy for prevention and treatment of type 1 diabetes.

RESEARCH DESIGN AND METHODS

A B6.129S2-*Alox15*^{tm1Fun} male mouse, kindly provided by Dr. Colin Funk (Department of Physiology, Queen's University, Kingston, Ontario, Canada) (37), was mated with an NOD female, followed by successive backcrosses to NOD males in a "speed congenic" strategy using mapped polymorphic microsatellites for genotypic selection (panel available upon request to M.M.). The NOD mice used in this study were obtained from a breeding nucleus at the Barbara Davis Center for Childhood Diabetes (Denver, CO) and have been propagated at the University of Virginia by brother-sister mating since 1993. All mice are bred and maintained in a pathogen-free colony in the Center for Comparative Medicine under protocols approved by the institutional animal care and use committee using American Association for Accreditation of Laboratory Animal Care guidelines.

Genotyping

High-quality genomic DNA was prepared from tail or liver by standard methods. For all microsatellite analysis, oligonucleotide pairs for mapped loci were used to amplify sequence-specific genomic DNA using a modification of published methods (38). For whole-genome scans, fluoro-chrome-labeled primers were synthesized using oligonucleotide sequences from the public domain (38). Fluor-labeled amplicons were pooled into multiplex sets and analyzed on an automated ABI sequencer using Genescan and Genotyper software (Applied Biosystems, Foster City, CA). For analysis of individual loci, PCR products amplified with unlabeled primers were separated on a 4% agarose gel and visualized with ethidium bromide. The mutant *Alox15* allele was genotyped during backcross breeding using a standard set of primers recognizing a retained neomycin-resistance cassette, using published primer sequences and protocol (IMR0013: 5′-CTTGGGTGGAGAGGCTATTC-3′ and IMR0014: 5′-AGGTGAGATGACAGGAGATC-3′; protocol available from http://www.jax.org/imr/touchdown.html).

For allele-specific genotyping of *Alox15*, PCR was performed using the following primers: CDF 141: 5′-ATC GCC TTC TTG ACG AGT TC; CDF 233: 5′-TCC TGA ACA GGC CTT GAG AG; and CDF 234: 5′-GAG GGC ACT GGT GAG CAG A (37,39). PCR was performed for 35 cycles using an annealing temperature of 65°C. Products were separated on 1% agarose gel and visualized with ethidium bromide. The mutant allele yields a 700-bp fragment, indicating disruption of *Alox15*, while a 350-bp fragment is generated from the wild-type allele.

Determination of disease status

Mice at risk for development of diabetes were screened for polyuria and morning glycosuria beginning at 10 weeks of age. Individuals with urine glucose concentrations >500 mg/dl twice at 24-h intervals received 0.5 units per day of human Ultralente insulin. After 7 consecutive days of insulin requirement, diabetes was confirmed with a blood glucose measurement using an UltraTouch glucometer (Lifescan, Milpitas, CA). All mice that required insulin for 7 consecutive days had blood glucose concentrations >300 mg/dl. Mice

exhibiting no glycosuria by 210 days of age were killed for pancreatic histology after confirmation of normoglycemia (morning blood glucose <140 mg/dl).

Macrophage isolation and detection of 12/15 LO by immunobloting and real-time PCR

Male NOD-*Alox15*^{null} and NOD mice (6–8 months old) were injected with sterile 4% thioglycollate; after 72 h, cells were pelleted from ascites, washed with RPMI-1640 medium containing 10% FBS and 100 μ/ml penicillin/streptomycin containing EDTA, and cultured for 3 h at 37°C in 5% CO_2. Nonadherent cells were removed by multiple washes with Hank's buffered saline. Adherent cells were washed with 10% nonheated FBS and incubated for 2 days with a second wash to remove nonadherent cells after 24 h. Protein was isolated using CelLytic M Cell Lysis reagent (Sigma, St. Louis, MO).

For quantitation of 12/15-LO protein, cell lysates from two mice from each strain were pooled and proteins separated by electrophoresis on a 10% polyacrylimide gel (50 μg protein per lane). Actin was used as loading control. Primary antibodies were 12/15-LO polyclonal rabbit, affinity purified A2460, and BLD B&4 (used at 1:2,500; synthesized in the Nadler laboratory). Polyclonal rabbit anti-mouse actin (1:2,500; Santa Cruz Biotechnology, Santa Cruz, CA) was used as loading control. Secondary antibody was anti-rabbit IgG-HRP (1:5,000; Santa Cruz Biotechnology).

RNA was isolated from 4% thioglycolate-stimulated peritoneal macrophages according to Qiagen RNeasy Mini kit instructions (including an optional DNase step) right after the completion of incubation period. PCR was performed on Stratagene MX3000P with MxPro Version 3 software, using the following 12/15-LO primers: forward, 5′-CTCTCAAGGCCTGTTCAGGA-3′; reverse, 5′-GTCCATTGTCCCCAGAACCT-3′, with annealing temperature 62°C and extension temperature of 72°C and final extension of 81°C (40). The concentration of β-actin (forward, 5′- AGAGGGAAATCGTGCGTGAC-3′; reverse, 5′-CAATAGTGATGACCTGGCCGT-3′, with annealing temperature of 62°C) was no different between the samples from the two strains.

Metabolic testing

For testing glucose tolerance, mice were fasted overnight and then injected intraperitoneally with glucose (2 g/kg). Blood glucose measurements were performed with an UltraTouch glucometer using blood samples taken from cut tail tips at baseline and at 10, 20, 30, 60, 90, and 120 min after the injection of glucose. Fasting plasma insulin was measured in blood obtained from tail veins after an overnight fast using a commercial insulin radioimmune assay (catalog no. SRI-13K; Linco Research, St. Charles, MO). Plasma was also collected during intraperitoneal glucose tolerance test at baseline and at 10 and 30 min for insulin measurements using Ultrasensitive Rat/Mouse Insulin ELISA (Crystal Chem, Downers Grove, IL). Homeostasis model assessment was calculated using the following formula: [fasting insulin (μU/ml) × fasting blood glucose (mmol/l)]/22.5.

Histological scoring for insulitis

Whole pancreas was spread onto plastic cassettes and fixed for 24 h in 10% buffered formalin before automated processing and embedding in paraffin. Consecutive 4 μmol/l sections (three per slide) were stained with aldehyde fuchsin and hematoxylin. A single score, indicating average severity of insulitis, was given for each mouse based on evaluation of all islets identified by morphology using the following scale: 0, no infiltrate; 1, polar infiltrate only; 2, infiltrating cells extending around islet to >50% of its circumference without invasion; and 3, invasive insulitis. A β-cell score was determined as a product of the residual total islet mass, estimated as a fraction of that in age- and sex-matched NOD.scid control mice (0.0–1.0) multiplied by the average percentage of aldehyde fuchsin–positive

cells per islet relative to control (0–100%). Adjunct perivascular and periductular infiltrates, indicative of total pancreatic inflammation, were also compared using a score of 0 (no evidence of mononuclear cell infiltrate) to 3 (extensive infiltrates associated with pancreatic ducts and blood vessels, independent of local islet tissue, and characterized by displacement of exocrine tissue and engorgement of lymphatics) (41).

Immunofluorescence and immunohistochemistry

Five-micron sections from flash-frozen pancreas were fixed in a 1:1 mixture of 100% ethanol and acetone, followed by blocking of endogenous biotin. For CD4, sections were incubated in rabbit anti-insulin (1:25 in 2% goat serum; Santa Cruz Biotechnology), followed by amplification with a biotinylated goat anti-rabbit antibody (1:200; Vector Laboratories, Burlingame, CA) and Texas Red–labeled Neutralite-Avidin (1:300; SouthernBiotech, Birmingham, AL) or with FITC-labeled anti-CD4 (1:150; BD Biosciences, San Jose, CA) amplified using the Tyramide FITC amplification system (Perkin Elmer, Waltham, MA). To visualize islet-associated Foxp3, sections were stained for insulin using rabbit anti-insulin as described above, followed by Cy2-labeled goat anti-rabbit (1:50; Jackson ImmunoResearch, West Grove, PA). Sections were then incubated with biotin anti-mouse Foxp3 (1:100; eBiosciences, San Diego, CA), followed by amplification with the Tyramide Biotin amplification system (Perkin Elmer) coupled with Texas Red–labeled Neutralite-Avidin. All sections were stained with Hoechst Dye (5 μg/ml; Invitrogen, Carlsbad, CA) to visualize nuclei. Stained sections were viewed and photographed on an Olympus BX51WI fluorescence microscope (Olympus, Tokyo, Japan). Excitation light was supplied to the sections by a xenon burner through a filter wheel containing DAPI, FITC, and TRITC filters (Sutter Instrument Company, Novato, CA). Images were taken using a Hamamatsu ORCA-ER monochrome charged-coupled device camera (Hamamatsu Photonics, Iwata City, Japan). Data were acquired with IPLab software, version 4.0 (Scanalytics, Rockville, MD), and analyzed in NIH Image J (National Institutes of Health, Bethesda, MD).

For Mac-2 staining, pancreata from 4-week-old NOD and NOD-*Alox15*^{null} mice were fixed with 4% paraformaldehyde by heart perfusion. Tissues were dissected and incubated an additional 1 h in 4% paraformaldehyde, dehydrated in 70% ethanol, and embedded in paraffin. Nonspecific background was eliminated by 30-min incubation in methanol with 0.5% hydrogen peroxide, followed by blocking for 1 h in PBS containing 10% normal rabbit serum and avidin/biotin blocking reagent (Vector Laboratories). Activated macrophages were identified using rat anti-mouse Mac-2 (1:20,000; Accurate Chemical, Westbury, NY), followed by biotinylated anti-rat (mouse adsorbed) IgG (1:200; Vector Laboratories) and Vecstatin Elite (Vector Laboratories) avidin-biotin–horseradish peroxidase reagent. Bound antibody complexes were visualized with diaminobenzedine hydrochloride in 0.02% hydrogen peroxide. Negative controls were prepared by substituting rabbit IgG for the primary antibody. Slides were scored in blind fashion, using the following criteria: 0, no macrophage staining; 0.5, some staining in islet periphery; 1, one to three macrophages inside islet; 2, four or more macrophages; and 3, infiltration of >10% of islet surface.

Statistical analysis

Survival comparisons were analyzed by log-rank test using MedCalc for Windows, version 9.2.1.0. Results from glucose tolerance tests were compared using a two-way ANOVA to compare blood glucose differences with respect to factors of time and mouse strain. Insulin levels during a glucose tolerance test were compared using an unpaired one-tailed *t* test. Histological scores were compared using an unpaired two-tailed *t* test.

RESULTS

Generation of congenic NOD-B6;129S2-Alox15^{tm1fun} mice

A single founder B6;129S2-*Alox15*^{tm1Fun} male homozygote (~13% 129S2) (37) was mated to NOD females. Using a panel of 106 informative microsatellites, covering all chromosomes except Y, breeding females were selected for minimal residual donor genome during four successive generations of backcross to NOD males. Selection for the primary *Alox15* mutation was made using a retained neomycin-resistance cassette. To limit the flanking non-NOD alleles, mice from one additional backcross generation (n = 39) were selected for a minimal congenic interval, followed by intercross with further selection for flanking microsatellite loci (n = 86). The final line carries a non-NOD donor interval, including undefined regions, extending from *D11Mit177* to *D11Mit245* (65.0–76.7 Mb; NCBI, build m36) (Fig. 1*A*). It overlaps the intervals defining *Idd4.1* in the C57BL/6 and NOR congenic strains (Fig. 1*B*) but carries NOD alleles at *Il12b* and *Stat5b* (Fig. 1*A*), as well as *Idd4.3* (6) (Fig. 1*B*). *Alox15* itself clearly resides in the *Idd4.1* genetic interval and can be considered a regional candidate gene for *Idd4.1*. The remainder of the non-NOD interval in the final NOD-*Alox15*^{null} congenic strain, including the entire *Idd4.1* interval, is derived from the 129S2 genetic background.

Diabetes incidence in NOD-*Alox15*^{null} mice

The cumulative incidence of diabetes in this congenic line is markedly decreased from that in contemporary cohorts of NOD mice (Fig. 2*A* and *B*), with only 1 of 40 female NOD-*Alox15*^{null} homozygotes and 0 of 33 males becoming diabetic by 7 months of age (P < 0.0001 and <0.002 for females and males, respectively, by log-rank test). For females, the hazard ratio for diabetes is <0.00005 (95% CI 0.0137–0.1095). This contrasts with a published cumulative incidence of diabetes of 15% (3 of 20) in female NOD.B6*Idd4a* mice (carrying the entire *Idd4.1–4.2* interval from C57BL/6 mice) (Fig. 1*B*) (7) and 60% (21 of 35) in female NOD.Nor-*Idd4* (long) mice carrying a protective interval from the NOR strain (42).

Absence of *Alox15* gene expression in NOD-*Alox15*^{null} macrophages

We confirmed the absence of 12/15-LO with both RT-PCR and immunoblotting in macrophages from thioglycollate-elicited peritoneal exudates. As expected, we found high levels of 12/15-LO protein in cells from NOD mice, while it is undetectable NOD-*Alox15*^{null}. Similarly, we found no evidence of residual mRNA expression using primers spanning intron 2; Fig. 2*D* shows a 750-fold difference in 12/15-LO mRNA abundance between the two strains.

Glucose tolerance test

12/15-LO is expressed at high levels in pancreatic islets, but its normal role in this tissue is unknown. To determine whether pancreatic β-cells were less responsive in the absence of 12/15-LO activity, we challenged 8-month-old nondiabetic female NOD and NOD-*Alox15*^{null} mice with an intraperitoneal glucose tolerance test. As is shown in Fig. 3, NOD-*Alox15*^{null} mice cleared glucose more efficiently than NOD mice. Blood glucose values over the entire time course of the test were lower in the NOD-*Alox15*^{null} mice compared with nondiabetic NOD controls (P < 0.0001 by two-way ANOVA). This result suggested that the NOD-*Alox15*^{null} mice were either more insulin sensitive or maintained better β-cell function than NOD mice. Mean fasting blood glucose and insulin levels were similar in the NOD-*Alox15*^{null} and in the NOD controls (Table 1), resulting in a similar homeostasis model assessment index (a measure of insulin sensitivity) between the two strains. However, while insulin levels peaked at 10 min in both groups, peak insulin concentration was significantly

higher in NOD-*Alox15*^{null} mice than in the NOD group (0.87 ± 0.117 vs. 0.39 ± 0.194 ng/ml, $P = 0.04$), consistent with better preservation of islet mass and function in older mice from the congenic strain.

Severity of insulitis in NOD-*Alox15*^{null} mice

As expected, based on improved insulin production in NOD-*Alox15*^{null} mice after an intraperitoneal glucose tolerance test, pancreatic histology in nondiabetic NOD-*Alox15*^{null} females at 30 weeks of age showed a marked reduction in both invasive insulitis and β-cell damage compared with age-matched nondiabetic NOD females. A representative pancreatic section from an NOD-*Alox15*^{null} female mouse is shown in Fig. 4*A* and demonstrates significant perivascular/periductular mononuclear cell inflammation but no evidence of invasive insulitis. This contrasts with a representative section from an age-matched nondiabetic female NOD mouse, showing a heavily infiltrated islet with loss of β-cell insulin granules (Fig. 4*B*). Islet-associated infiltrates in NOD-*Alox15*^{null} mice were almost exclusively limited to polar accumulations of mononuclear cells (average score per pancreas <1.0, on a scale of 0–3), while islets from surviving nondiabetic NOD females at 30 weeks showed invasive insulitis (average score >2.5; $P < 0.001$) (Table 2).

Perivascular/periductular inflammation was seen in both strains at this age, but the extent of these infiltrates was significantly decreased in congenic mice (Table 2). Both the residual islet mass and the intensity/extent of aldehyde fuchsin–positive islet cells were well preserved in NOD-*Alox15*^{null} females relative to age-matched nondiabetic NOD females, producing a significantly increased score for β-cell preservation in the NOD-*Alox15*^{null} mice ($P < 0.001$).

Recruitment of CD4$^+$ T cells and Foxp3$^+$ regulatory T-cells in NOD-*Alox15*^{null} mice

CD4$^+$ cells were also markedly decreased in pancreatic sections from NOD-*Alox15*^{null} mice. At 9.5 weeks, CD4 staining was much more prevalent in NOD mice (Fig. 5*A*) than NOD-*Alox15*^{null} mice (Fig. 5*B*). By ~30 weeks of age, we observed accumulations of CD4$^+$ T cells near islets from both NOD and NOD-*Alox15*^{null} mice (Fig. 5*C* and *D*). However, many more islets were observed in sections from NOD-*Alox15*^{null} mice (66 islets from two NOD-*Alox15*^{null} mice vs. 16 in two NOD mice), and a larger percentage of these islets showed no signs of insulitis (~50% of NOD-*Alox15*^{null} islets vs. ~10% of NOD islets). Since increased development and accumulation of regulatory T-cells might provide a mechanism for decreasing both the extent and destructiveness of islet-associated inflammation in NOD-*Alox15*^{null} mice, we stained sections from 30-week-old mice for Foxp3. Foxp3 is a transcription factor involved in the development of regulatory T-cells and is used as a marker for identifying these cells. As shown in Fig. 5*E*, very little Foxp3 staining was typically observed among islets from NOD mice, whereas substantial numbers of Foxp3$^+$ cells were observed among NOD-*Alox15*^{null} islets with signs of insulitis (Fig. 5*F*). Foxp3$^+$ cells were generally not observed in or near pancreatic islets in the absence of insulitis in either strain (data not shown).

Macrophage infiltration in 4-week-old NOD-*Alox15*^{null} mice

Early islet invasion by macrophages is a characteristic feature of disease process in NOD mice and precedes accumulation of lymphocytes (18). Since 12/15-LO has been shown to enhance macrophage activation, we postulated that a decrease in the presence of activated macrophages associated with pancreatic islets might be responsible for the reduced severity of insulitis along with an increase in cells with apparent regulatory function in NOD-*Alox15*^{null} mice. Pancreata from 4-week-old female mice, before the development of detectable pancreatic T-cell infiltration in the NOD controls, were stained for the macrophage activation marker, Mac-2. Figure 6 shows representative examples of islets

from the two strains, with brown staining signifying infiltration with activated macrophages. Using a blinded scoring system, we found islet-associated Mac-2–positive macrophages in or around 36% of islets (20 of 56) from NOD-*Alox15*^{null} mice, whereas 65% of NOD islets (62 of 96) were Mac-2 positive ($P < 0.001$). This difference is also reflected in the mean Mac-2 score for each group: NOD 0.833 ± 0.075; NOD-*Alox15*^{null} 0.55 ± 0.097, $P = 0.02$), indicating greater intra-islet accumulation of Mac-2–positive cells in pancreatic sections from NOD mice.

DISCUSSION

Our previous studies had demonstrated that targeted deletion of 12/15-LO in mice with a largely C57BL/6 genetic background resulted in protection from streptozotocin-induced β-cell destruction (36). In this study, we show that deletion of 12/15-LO activity via a congenic strategy is also associated with a decrease in autoimmune diabetes in NOD mice. This finding suggests that 12/15-LO may play a direct role in the development of diabetes in this strain.

As noted in the introduction, *Alox15* resides within a previously identified diabetes susceptibility locus, *Idd4.1*, on mouse chromosome 11. Danska and colleagues (42) have recently published an elegant and comprehensive analysis of gene expression in the *Idd4.1* interval using NOR.NOD-*Idd4* congenic mouse lines. In these mice, segments of NOD chromosome 11 near *Idd4.1* (Fig. 1*B*) introduced an increase in spontaneous, as well as cyclo-phosphamide-accelerated, diabetes when they were bred onto the normally diabetes-resistant NOR genetic background, which itself is a complex mixture of DBA/2, C57BL/Ks, and NOD. Following demonstration that the *Idd4.1* interval carries alleles from the nondiabetes-prone DBA/2 strain in NOR mice, they used microarray expression analysis to identify regional genes with differential expression in NOR and NOD mouse bone marrow–derived macrophages. Eleven of 52 regional genes were differentially expressed in these strains. Of these genes, the NOD and DBA/2 alleles of *Alox15* and the closely linked gene *Psmb6*, encoding a proteosome component, were also shown to differ in both potential regulatory sequence and predicted amino acid sequence, suggesting that they should be considered the primary regional candidates for controlling diabetes susceptibility in NOR mice. Interestingly, however, comparative sequencing showed that the NOD and C57BL/6 *Alox15* alleles appear to be identical at the genomic level. This observation makes it unlikely that this locus is responsible for *Idd4* loci mapped using crosses with C57BL/6 mice studied by Delovitch and colleagues (7) (Fig. 1*B*) or the original genetic mapping with C57BL/10 (6). Furthermore, *Alox15* mRNA is actually increased in disease-resistant NOR mice relative to the diabetes-prone congenic strains, suggesting that any differential effects of 12/15-LO in the NOR congenic strains operates by a different mechanism than that in our 12/15-LO–deficient strain.

All of the models generated to identify specific diabetes susceptibility loci on chromosome 11, including ours, have used a congenic strategy because of the lack of NOD-derived embryonic stem cells that are competent for homologous recombination with germ-line transmission of induced mutations. The use of congenic mice inevitably imposes constraints on the interpretation of differences in complex phenotypes, such as autoimmune diabetes, because of the extended regions of allelic variation flanking the gene or locus of primary interest. Even with careful attention to generation of a pure NOD genetic background, it is clearly possible that non-NOD alleles of more than one gene in the interval flanking the target gene could modify the incidence of diabetes in a congenic strain. During our congenic derivation, we had initially isolated, and bred to homozygosity, a larger fragment from the donor strain that carried both 129S2 and B6 alleles within the 50-Mb interval bounded by *D11Mit84* (34.4 Mb, mNCBI 36) and *D11Mit33* (81.6 Mb). In these mice, 129S2 alleles

extended from the centromeric end of the interval to a recombination point between *D11Mit320* and *D11Mit364* (70.8 and 72.0 Mb, respectively) with the remaining interval derived from the B6 strain. Homozygous *Alox15*^{null} congenic mice carrying this longer interval had only a modest decrease in the incidence of diabetes (46% of 41 females observed to 30 weeks of age, compared with an incidence of 65% in a contemporary cohort of NOD female mice). A similar incidence was observed in a small group of mice homozygous for a shorter fragment consisting only of 129S2-derived alleles flanked by *D11Mit84* and *D11Mit364* (four of eight females). In both of these lines, disease incidence in congenic males was modestly decreased relative to that in NOD males (17% for congenic mice vs. 25% for NOD). Taken together with the markedly lower incidence observed in the final NOD-*Alox15*^{null} line presented in this report, these results strongly suggest that a 129S2-derived susceptibility allele is present for at least one gene in the 30-Mb interval extending from *D11Mit84* to *D11Mit113*. However, we still cannot rule out the possibility that the disease resistance conferred by the smaller congenic interval is enhanced by non-NOD alleles at genes tightly linked but telomeric to *Alox15*.

One regional gene that might be postulated to complicate interpretation of disease susceptibility in our mice is the gene encoding the capsaicin receptor, *Trpv1* (73.0 Mb), which lies within the congenic interval in our strain (Fig. 1*A*). *Trpv1* was recently shown to be polymorphic in NOD mice when compared with B6 (43). Destruction of capsaicin-sensitive neurons in NOD mice protected them from severe invasive insulitis and resulted in improved insulin sensitivity. Furthermore, replacement of the NOD *Trpv1* allele with that from the B6 strain using congenic NOD.B6-*Idd4* mice produced phenotypes similar to those seen in capsaicin-treated NOD mice, leading these investigators to suggest that this gene may be a good candidate for the *Idd4.1* locus mapped using crosses between these two strains.

Based on microsatellite mapping, the *Trpv1* allele present in our final NOD congenic strain is derived from the C57BL/6 mouse and, therefore, must be considered a potential confounding factor in these studies. However, there remains significant controversy about the relationship of *Trpv1* variants to the development of diabetes in NOD mice (44). While a decrease in insulitis and diabetes was seen after capsaicin treatment of NOD mice, functional abnormalities in the treated mice were limited to demonstrations of insulin resistance and poor calcium flux in neurons. Attempts to link *Trpv1* variants directly to autoimmune diabetes using the NOD-*Idd4* mouse strains produced by Grattan et al. (7) are complicated by the recent demonstration that these strains are contaminated by C57BL/6 alleles across the powerful *Idd5* interval on chromosome 1 (45). Thus, direct evidence that *Trpv1* participates in protecting these mice from autoimmune diabetes is lacking. Dissection of our congenic interval by further recombination will be required to determine whether *Trpv1* may contribute to the striking diabetes resistance in our congenic strain. This effort will be complemented by analysis of disease susceptibility in NOD-*Idd4* mice lacking contaminating C57BL/6 alleles at the loci contributing to *Idd5* that are currently under construction at the Type 1 Diabetes Repository (E.H. Leiter, personal communication).

To begin to determine the mechanism(s) by which diabetes is prevented in NOD-*Alox15*^{null} congenic mice, we studied the role of several key immune cells involved in the infiltration of the pancreatic islets over the course of diabetes pathogenesis. Insulitis in NOD mice is initiated by infiltration of antigen-presenting cells, such as macrophages and dendritic cells (18). Our data show that 4-week-old female NOD-*Alox15*^{null} mice carry markedly reduced macrophage numbers in and around the islets compared with age-matched NOD female controls. The mechanism for this reduction in islet-associated macrophages is not clear. However, accumulating evidence suggests that the 12/15-LO product, 12(S)-HETE, can upregulate proinflammatory cytokine and chemokine production in macrophages. In

preliminary studies, we evaluated selected proinflammatory cytokine and chemokine levels, including monocyte chemoattractant 1 and the central proinflammatory cytokine IL-12, in thioglycollate-induced peritoneal macrophages using quantitative RT-PCR. Monocyte chemoattractant 1, which recruits macrophages and other hematopoietic lineages to sites of inflammation, was increased by 85% in NOD macrophages relative to those from NOD-*Alox15*^{null} mice. Similarly, IL-12p40 was highly expressed in NOD macrophages but virtually undetectable in the knockout strain, suggesting that both macrophage migration and activation were likely to be defective in these mice (N.A.M., unpublished observations).

Once insulitis has been established in NOD mice, several lines of evidence suggest that β-cell damage leading to insulin deficiency occurs in parallel with decreases in the number and/or function of Foxp3^{+} regulatory T-cells (rev. in 46). Although we found that CD4^{+} T cells are strikingly decreased in the pancreas of NOD-*Alox15*^{null} mice, these mice exhibit increased numbers of Foxp3^{+} cells in the peri-islet infiltrates. This observation suggests that the absence of 12/15-LO activity may allow enhanced production and recruitment of regulatory T-cells to the pancreas while limiting the recruitment of potential effector cells. In ongoing studies, we are investigating the possibility that enhanced regulatory cell activity can be linked to altered macrophage function in these congenic mice.

The pathways regulating 12/15-LO expression in islets or macrophages are complex and incompletely characterized. As previously noted, increased 12/15-LO activity enhances production of IL-12 in macrophages (15), consistent with a predominantly Th1-type activity associated with disease in NOD mice. IL-4, a T-cell–derived cytokine, is commonly associated with Th2 or protective responses in autoimmunity through its suppressive action on antigen-presenting cells such as B-lymphocytes or macrophages. However, IL-4 has been shown to increase 12/15-LO expression in mice (47). Taken together with the protective effects of deleting 12/15-LO in our study, this poses a potential conundrum. However, the link between IL-4 responses and proinflammatory IL-12 production through 12/15-LO is consistent with the observation that transgenic NOD mice expressing high levels of IL-4 under the control of the rat insulin promoter actually show increased inflammation and enhancement of islet-specific effector T-cell function (48). IL-4 does appear to decrease the severity of experimental allergic encephalomyelitis (EAE), a rodent model of multiple sclerosis (49), possibly accounting for the report that deletion of 12/15-LO exacerbates EAE in mice (50). We speculate that the protective action of 12/15-LO in the NOD mouse model of type 1 diabetes is due to the important role of IL-12 in type 1 diabetes, in contrast to the critical role of IL-23 (and not IL-12) for the induction of EAE (51). Whether 12/15-LO activity in pancreatic β-cells also contributes to the development of insulitis and diabetes remains to be determined (52,53).

In summary, data from the NOD-*Alox15*^{null} mouse suggest an important role for 12/15-LO in conferring susceptibility to autoimmune diabetes in NOD mice. The demonstration that islet-associated activated macrophages are markedly decreased in NOD-*Alox15*^{null} mice before the onset of significant infiltration by T-lymphocytes strongly suggests that 12/15-LO, or one of its products, is essential for disease initiation through its proinflammatory effects on macrophages, perhaps leading to decreased recruitment and/or survival of Foxp3^{+} regulatory cells. Whether or not the human homolog can be shown to play a role in disease susceptibility, we postulate that pharmacological blockade of either 12/15-LO activity or signaling downstream of a 12/15-LO–derived lipid mediator could provide a new approach to protecting β-cells from immune injury through alterations in the selective recruitment of regulatory versus effector cells. There are currently no compounds available for testing in vivo that specifically inhibit 12/15-LO and have a favorable long-term toxicity profile (54,55). However, the data presented in this study would suggest a possible clinical role for a specific and safe 12/15-LO inhibitor for use in clinical trials.

Acknowledgments

This work was supported by the following grants: National Institutes of Health RO1 DK55240; DERC and Animal Characterization Core and Cell and Islet Isolation Core Facilities at UVA Grant DK063609; and Institutional Diabetes Training Grant DK007320-29. This work also received funding from the American Diabetes Association, the Ella Fitzgerald Charitable Foundation, and the Iacocca Foundation.

Glossary

EAE	experimental allergic encephalomyelitis
HETE	hydroxyeicosatetranoic acid
IL	interleukin

REFERENCES

1. Atkinson MA, Leiter EH. The NOD mouse model of type 1 diabetes: as good as it gets? Nat Med 1999;5:601–604. [PubMed: 10371488]
2. Maier LM, Wicker LS. Genetic susceptibility to type 1 diabetes. Curr Opin Immunol 2005;17:601–608. [PubMed: 16226440]
3. Todd JA, Aitman TJ, Cornall RJ, Ghosh S, Hall JR, Hearne CM, Knight AM, Love JM, McAleer MA, Prins JB. Genetic analysis of autoimmune type 1 diabetes mellitus in mice. Nature 1991;351:542–547. [PubMed: 1675432]
4. Ivakine EA, Fox CJ, Paterson AD, Mortin-Toth SM, Canty A, Walton DS, Aleksa K, Ito S, Danska JS. Sex-specific effect of insulin-dependent diabetes 4 on regulation of diabetes pathogenesis in the nonobese diabetic mouse. J Immunol 2005;174:7129–7140. [PubMed: 15905556]
5. McDuffie M. Derivation of diabetes-resistant congenic lines from the nonobese diabetic mouse. Clin Immunol 2000;96:119–130. [PubMed: 10900159]
6. Litherland SA, Grebe KM, Belkin NS, Paek E, Elf J, Atkinson M, Morel L, Clare-Salzler MJ, McDuffie M. Nonobese diabetic mouse congenic analysis reveals chromosome 11 locus contributing to diabetes susceptibility, macrophage STAT5 dysfunction, and granulocyte-macrophage colony-stimulating factor overproduction. J Immunol 2005;175:4561–4565. [PubMed: 16177100]
7. Grattan M, Mi QS, Meagher C, Delovitch TL. Congenic mapping of the diabetogenic locus Idd4 to a 5.2-cM region of chromosome 11 in NOD mice: identification of two potential candidate subloci. Diabetes 2002;51:215–223. [PubMed: 11756344]
8. Ivakine EA, Mortin-Toth SM, Gulban OM, Valova A, Canty A, Scott C, Danska JS. The idd4 locus displays sex-specific epistatic effects on type 1 diabetes susceptibility in nonobese diabetic mice. Diabetes 2006;55:3611–3619. [PubMed: 17130511]
9. Davoodi-Semiromi A, Laloraya M, Kumar GP, Purohit S, Jha RK, She JX. A mutant Stat5b with weaker DNA binding affinity defines a key defective pathway in nonobese diabetic mice. J Biol Chem 2004;279:11553–11561. [PubMed: 14701862]
10. Laloraya M, voodi-Semiromi A, Kumar GP, McDuffie M, She JX. Impaired Crkl expression contributes to the defective DNA binding of Stat5b in nonobese diabetic mice. Diabetes 2006;55:734–741. [PubMed: 16505237]
11. Ymer SI, Huang D, Penna G, Gregori S, Branson K, Adorini L, Morahan G. Polymorphisms in the Il12b gene affect structure and expression of IL-12 in NOD and other autoimmune-prone mouse strains. Genes Immun 2002;3:151–157. [PubMed: 12070779]
12. Chen XS, Kurre U, Jenkins NA, Copeland NG, Funk CD. cDNA cloning, expression, mutagenesis of C-terminal isoleucine, genomic structure, and chromosomal localizations of murine 12-lipoxygenases. J Biol Chem 1994;269:13979–13987. [PubMed: 8188678]
13. Chen M, Yang ZD, Smith KM, Carter JD, Nadler JL. Activation of 12-lipoxygenase in proinflammatory cytokine-mediated beta cell toxicity. Diabetologia 2005;48:486–495. [PubMed: 15729574]

14. Soberman RJ, Harper TW, Betteridge D, Lewis RA, Austen KF. Characterization and separation of the arachidonic acid 5-lipoxygenase and linoleic acid omega-6 lipoxygenase (arachidonic acid 15-lipoxygenase) of human polymorphonuclear leukocytes. J Biol Chem 1985;260:4508–4515. [PubMed: 3920219]
15. Yamamoto S, Nishimura M, Conners MS, Stoltz RA, Falck JR, Chauhan K, Laniado-Schwartzman M. Oxidation and keto reduction of 12-hydroxy-5,8,10,14-eicosatetraenoic acids in bovine corneal epithelial microsomes. Biochim Biophys Acta 1994;1210:217–225. [PubMed: 8280773]
16. Jarpe AJ, Hickman MR, Anderson JT, Winter WE, Peck AB. Flow cytometric enumeration of mononuclear cell populations infiltrating the islets of Langerhans in prediabetic NOD mice: development of a model of autoimmune insulitis for type I diabetes. Reg Immunol 1990;3:305–317. [PubMed: 2132756]
17. Reddy S, Liu W, Elliott RB. Distribution of pancreatic macrophages preceding and during early insulitis in young NOD mice. Pancreas 1993;8:602–608. [PubMed: 8302797]
18. Charre S, Rosmalen JG, Pelegri C, Alves V, Leenen PJ, Drexhage HA, Homo-Delarche F. Abnormalities in dendritic cell and macrophage accumulation in the pancreas of nonobese diabetic (NOD) mice during the early neonatal period. Histol Histopathol 2002;17:393–401. [PubMed: 11962743]
19. Jansen A, Homo-Delarche F, Hooijkaas H, Leenen PJ, Dardenne M, Drexhage HA. Immunohistochemical characterization of monocytes-macrophages and dendritic cells involved in the initiation of the insulitis and β-cell destruction in NOD mice. Diabetes 1994;43:667–675. [PubMed: 8168644]
20. Rosmalen JG, Homo-Delarche F, Durant S, Kap M, Leenen PJ, Drexhage HA. Islet abnormalities associated with an early influx of dendritic cells and macrophages in NOD and NODscid mice. Lab Invest 2000;80:769–777. [PubMed: 10830787]
21. Rosmalen JG, Martin T, Dobbs C, Voerman JS, Drexhage HA, Haskins K, Leenen PJ. Subsets of macrophages and dendritic cells in nonobese diabetic mouse pancreatic inflammatory infiltrates: correlation with the development of diabetes. Lab Invest 2000;80:23–30. [PubMed: 10652999]
22. Serreze DV, Gaedeke JW, Leiter EH. Hematopoietic stem-cell defects underlying abnormal macrophage development and maturation in NOD/Lt mice: defective regulation of cytokine receptors and protein kinase C. Proc Natl Acad Sci U S A 1993;90:9625–9629. [PubMed: 8415751]
23. Langmuir PB, Bridgett MM, Bothwell AL, Crispe IN. Bone marrow abnormalities in the non-obese diabetic mouse. Int Immunol 1993;5:169–177. [PubMed: 8452815]
24. Alleva DG, Pavlovich RP, Grant C, Kaser SB, Beller DI. Aberrant macrophage cytokine production is a conserved feature among autoimmuneprone mouse strains: elevated interleukin (IL)-12 and an imbalance in tumor necrosis factor-α and IL-10 define a unique cytokine profile in macrophages from young nonobese diabetic mice. Diabetes 2000;49:1106–1115. [PubMed: 10909966]
25. Liu J, Beller DI. Distinct pathways for NF-kappa B regulation are associated with aberrant macrophage IL-12 production in lupus- and diabetes-prone mouse strains. J Immunol 2003;170:4489–4496. [PubMed: 12707325]
26. Maree AF, Komba M, Dyck C, Labecki M, Finegood DT, Edelstein-Keshet L. Quantifying macrophage defects in type 1 diabetes. J Theor Biol 2005;233:533–551. [PubMed: 15748914]
27. Nikolic T, Bunk M, Drexhage HA, Leenen PJ. Bone marrow precursors of nonobese diabetic mice develop into defective macrophage-like dendritic cells in vitro. J Immunol 2004;173:4342–4351. [PubMed: 15383563]
28. Stoffels K, Overbergh L, Giulietti A, Kasran A, Bouillon R, Gysemans C, Mathieu C. NOD macrophages produce high levels of inflammatory cytokines upon encounter of apoptotic or necrotic cells. J Autoimmun 2004;23:9–15. [PubMed: 15236748]
29. Nikolic T, Bouma G, Drexhage HA, Leenen PJ. Diabetes-prone NOD mice show an expanded subpopulation of mature circulating monocytes, which preferentially develop into macrophage-like cells in vitro. J Leukoc Biol 2005;78:70–79. [PubMed: 15788439]

30. O'Brien BA, Geng X, Orteu CH, Huang Y, Ghoreishi M, Zhang Y, Bush JA, Li G, Finegood DT, Dutz JP. A deficiency in the in vivo clearance of apoptotic cells is a feature of the NOD mouse. J Autoimmun 2006;26:104–115. [PubMed: 16431079]

31. Middleton MK, Rubinstein T, Pure E. Cellular and molecular mechanisms of the selective regulation of IL-12 production by 12/15-lipoxygenase. J Immunol 2006;176:265–274. [PubMed: 16365418]

32. Bleich D, Chen S, Gu JL, Thomas L, Scott S, Gonzales N, Natarajan R, Nadler JL. Interleukin-1 beta regulates the expression of a leukocyte type of 12-lipoxygenase in rat islets and RIN m5F cells. Endocrinology 1995;136:5736–5744. [PubMed: 7588331]

33. Ma Z, Ramanadham S, Corbett JA, Bohrer A, Gross RW, McDaniel ML, Turk J. Interleukin-1 enhances pancreatic islet arachidonic acid 12-lipoxygenase product generation by increasing substrate availability through a nitric oxide-dependent mechanism. J Biol Chem 1996;271:1029–1042. [PubMed: 8557627]

34. Bleich D, Chen S, Wen Y, Nadler JL. The stress-activated c-Jun protein kinase (JNK) is stimulated by lipoxygenase pathway product 12-HETE in RIN m5F cells. Biochem Biophys Res Commun 1997;230:448–451. [PubMed: 9016800]

35. Cyrus T, Witztum JL, Rader DJ, Tangirala R, Fazio S, Linton MF, Funk CD. Disruption of the 12/15-lipoxygenase gene diminishes atherosclerosis in apo E-deficient mice. J Clin Invest 1999;103:1597–1604. [PubMed: 10359569]

36. Bleich D, Chen S, Zipser B, Sun D, Funk CD, Nadler JL. Resistance to type 1 diabetes induction in 12-lipoxygenase knockout mice. J Clin Invest 1999;103:1431–1436. [PubMed: 10330425]

37. Sun D, Funk CD. Disruption of 12/15-lipoxygenase expression in peritoneal macrophages: enhanced utilization of the 5-lipoxygenase pathway and diminished oxidation of low density lipoprotein. J Biol Chem 1996;271:24055–24062. [PubMed: 8798642]

38. Dietrich WF, Miller J, Steen R, Merchant MA, Mron-Boles D, Husain Z, Dredge R, Daly MJ, Ingalls KA, O'Connor TJ. A comprehensive genetic map of the mouse genome. Nature 1996;380:149–152. [PubMed: 8600386]

39. George J, Afek A, Shaish A, Levkovitz H, Bloom N, Cyrus T, Zhao L, Funk CD, Sigal E, Harats D. 12/15-Lipoxygenase gene disruption attenuates atherogenesis in LDL receptor-deficient mice. Circulation 2001;104:1646–1650. [PubMed: 11581143]

40. Reilly KB, Srinivasan S, Hatley ME, Patricia MK, Lannigan J, Bolick DT, Vandenhoff G, Pei H, Natarajan R, Nadler JL, Hedrick CC. 12/15-Lipoxygenase activity mediates inflammatory monocyte/endothelial interactions and atherosclerosis in vivo. J Biol Chem 2004;279:9440–9450. [PubMed: 14676201]

41. Yang Z, Chen M, Ellett JD, Fialkow LB, Carter JD, McDuffie M, Nadler JL. Autoimmune diabetes is blocked in Stat4-deficient mice. J Autoimmun 2004;22:191–200. [PubMed: 15041039]

42. Ivakine EA, Gulban OM, Mortin-Toth SM, Wankiewicz E, Scott C, Spurrell D, Canty A, Danska JS. Molecular genetic analysis of the Idd4 locus implicates the IFN response in type 1 diabetes susceptibility in nonobese diabetic mice. J Immunol 2006;176:2976–2990. [PubMed: 16493056]

43. Razavi R, Chan Y, Afifiyan FN, Liu XJ, Wan X, Yantha J, Tsui H, Tang L, Tsai S, Santamaria P, Driver JP, Serreze D, Salter MW, Dosch HM. TRPV1+ sensory neurons control beta cell stress and islet inflammation in autoimmune diabetes. Cell 2006;127:1123–1135. [PubMed: 17174891]

44. Bour-Jordan H, Bluestone JA. Sensory neurons link the nervous system and autoimmune diabetes. Cell 2006;127:1097–1099. [PubMed: 17174888]

45. Leiter, EH.; The Jackson Laboratory. [Accessed 9 November 2006]. Available from http://www.jax.org/t1dr/images/5311_5312_5313_idd_sweep_and_chr1_and_11_scan.jpg

46. Bluestone JA, Tang Q. Therapeutic vaccination using CD4+CD25+ antigen-specific regulatory T cells. Proc Natl Acad Sci U S A 2004;101(Suppl. 2):14622–14626. [PubMed: 15322272]

47. Huang JT, Welch JS, Ricote M, Binder CJ, Willson TM, Kelly C, Witztum JL, Funk CD, Conrad D, Glass CK. Interleukin-4-dependent production of PPAR-gamma ligands in macrophages by 12/15-lipoxygenase. Nature 1999;400:378–382. [PubMed: 10432118]

48. Falcone M, Yeung B, Tucker L, Rodriguez E, Krahl T, Sarvetnick N. IL-4 triggers autoimmune diabetes by increasing self-antigen presentation within the pancreatic islets. Clin Immunol 2001;98:190–199. [PubMed: 11161975]

49. Ho SH, Lee HJ, Kim DS, Jeong JG, Kim S, Yu SS, Jin Z, Kim S, Kim JM. Intrasplenic electro-transfer of IL-4 encoding plasmid DNA efficiently inhibits rat experimental allergic encephalomyelitis. Biochem Biophys Res Commun 2006;343:816–824. [PubMed: 16564024]
50. Emerson MR, LeVine SM. Experimental allergic encephalomyelitis is exacerbated in mice deficient for 12/15-lipoxygenase or 5-lipoxygenase. Brain Res 2004;1021:140–145. [PubMed: 15328042]
51. Thakker P, Leach MW, Kuang W, Benoit SE, Leonard JP, Marusic S. IL-23 is critical in the induction but not in the effector phase of experimental autoimmune encephalomyelitis. J Immunol 2007;178:2589–2598. [PubMed: 17277169]
52. Bleich D, Chen S, Gu JL, Nadler JL. The role of 12-lipoxygenase in pancreatic-cells (Review). Int J Mol Med 1998;1:265–272. [PubMed: 9852229]
53. Wen Y, Gu J, Chakrabarti SK, Aylor K, Marshall J, Takahashi Y, Yoshimoto T, Nadler JL. The role of 12/15-lipoxygenase in the expression of interleukin-6 and tumor necrosis factor-alpha in macrophages. Endocrinology 2007;148:1313–1322. [PubMed: 17170102]
54. Im JY, Han PL. Nordihydroguaiaretic acid induces astroglial death via glutathione depletion. J Neurosci Res 2007;85:3127–3134. [PubMed: 17663482]
55. Fujimoto Y, Ikeda M, Sakuma S. Monochloramine potently inhibits arachidonic acid metabolism in rat platelets. Biochem Biophys Res Commun 2006;344:140–145. [PubMed: 16615995]

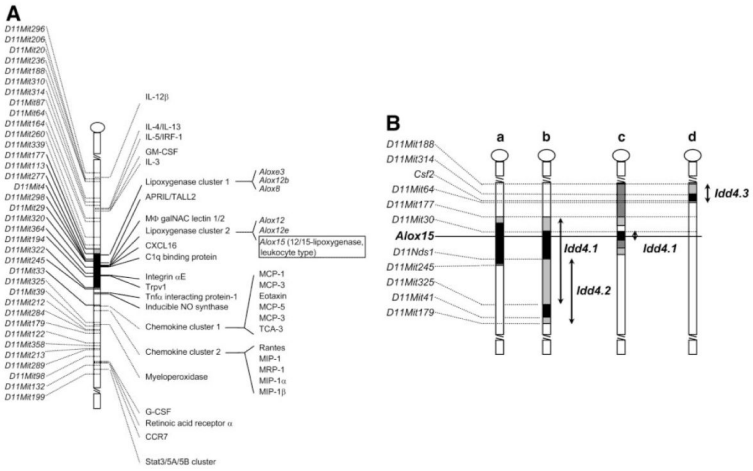

FIG. 1.

A: Location of the fragment introgressed to generate the NOD-*Alox15*^{null} congenic strain. Black intervals represent confirmed homozygosity for B6;129S2 from the donor B6,129S2-*Alox15*^{tm1Fun} strain; light gray intervals are indeterminate regions containing recombination end points for the congenic interval; and white intervals are regions derived from the congenic background strain. *B*: Intervals defining sub-loci for *Idd4* in congenic mouse strains. *a*: Map of NOD-*Alox15*^{null} mice (this report). *b*: Composite map from NOD-Idd4A and NOD-Idd4B (7), showing localization of *Idd4.1* and *Idd4.2*. *c*: Composite map of NOD contributions to informative NOR.NOD-*Idd4*R3 and NOR.NOD-*Idd4*R3 congenic lines (42). *d*: Map of NOD.Lc11b, showing localization of *Idd4*.3 (6). Black intervals represent confirmed homozygosity for donor alleles: B6;129S2 in panel *a*, B6 in panel *b*, NOD in panel *c*; white intervals, regions derived from the congenic background strain; light gray intervals, indeterminate regions containing recombination end points. In panel *c*, dark gray intervals represent known NOD-derived regions in informative congenic lines.

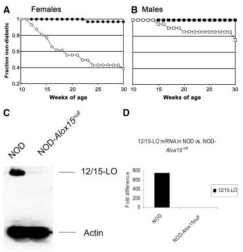

FIG. 2.

A and *B*: Disease incidence in NOD-*Alox15*^{null} mice compared with NOD mice. *A*: Females, *n* = 40; *B*: males, *n* = 34. Filled symbols: NOD-*Alox15*^{null}; open symbols: NOD. *C* and *D*: Confirmation of 12/15-LO functional deletion. Comparison of expression of 12/15-LO in peritoneal exudate macrophages from NOD and NOD-*Alox15*^{null} mice. Immunoblot (*C*) and real-time quantitative RT-PCR (*D*).

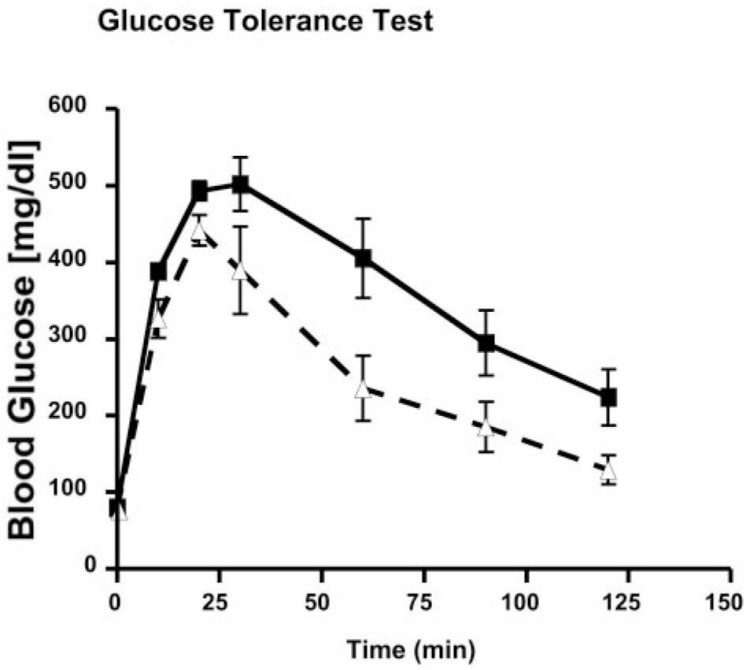

FIG. 3.

Glucose tolerance test results for NOD and NOD-*Alox15*^{null} mice. Female NOD (■, $n = 5$) and NOD-*Alox15*^{null} (△, $n = 5$) mice at 8 months of age were subjected to a glucose tolerance test. Data points represent mean blood glucose values ± SE. Differences in blood glucose levels were statistically significant over the entire test period ($P < 0.0001$ by two-way ANOVA).

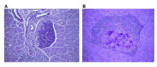

FIG. 4.

Aldehyde fuchsin staining of the islets. Fourteen nondiabetic female NOD-*Alox15*^{null} mice and 10 nondiabetic NOD females were evaluated for insulitis and β-cell granulation at 30 weeks of age. Pancreata were stained with aldehyde fuchsin and evaluated by standard light microscopy. *A*: Representative section showing a well-preserved islet in a NOD-*Alox15*^{null} mouse. *B*: A representative example of an infiltrated islet seen in an age-matched nondiabetic NOD mouse.

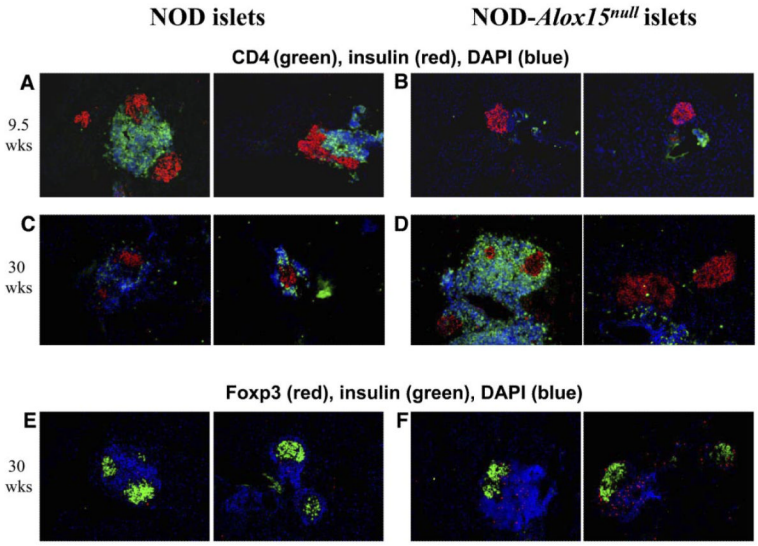

FIG. 5.

Immunofluorescent staining of frozen pancreatic sections from NOD and NOD-*Alox15*^{null} islets. Representative sections from 9.5-week-old NOD (*A*) or NOD-*Alox15*^{null} (*B*) mice, and ≥30-week-old NOD (*C*) or NOD-*Alox15*^{null} (*D*) mice were stained with antibodies against insulin (red) and CD4 (green), as well as Hoechst dye (blue, nuclear staining). Panels *E* (NOD) and *F* (NOD-*Alox15*^{null}) show representative sections from ≥30-week-old mice costained for insulin (green), Foxp3 (red), and Hoechst (blue).

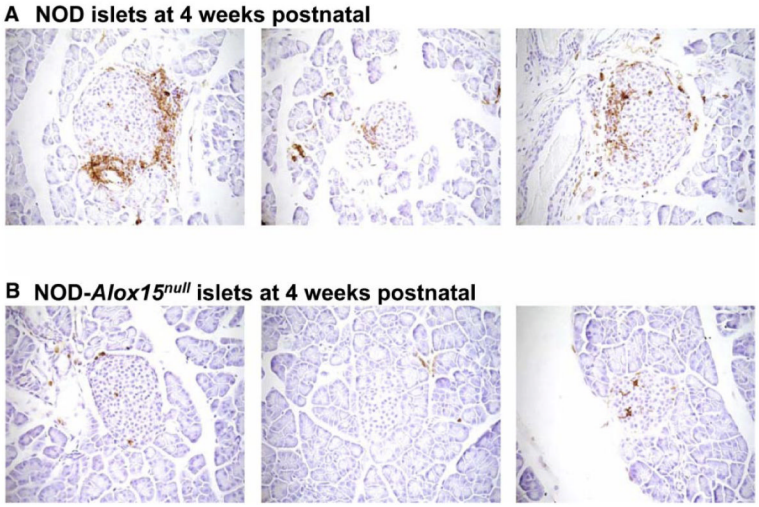

FIG. 6.

Islet-associated activated macrophages. Pancreata from 4-week-old NOD (*A*) and NOD-*Alox15*^{null} (*B*) mice were stained for Mac-2 (brown) and blindly scored for degree of infiltration. Sections shown are representative of the results from four individual mice from each strain.

TABLE 1

Fasting blood glucose and plasma insulin in NOD and NOD-*Alox15*^{null} mice

Genotype	n	Blood glucose (mg/dl)	Insulin (ng/ml)	HOMA
NOD	4	80 ± 6	0.13 ± 0.037	0.71 ± 0.165
NOD-*Alox15*^{null}	5	74 ± 10	0.17 ± 0.047	0.82 ± 0.208
P		0.622	0.559	0.713

Data are means ± SE. HOMA, homeostasis model assessment.

TABLE 2

Insulitis scores

Pancreatic histology	NOD	NOD-*Alox15*^{null}	P
Periductular infiltrate (range 0–3)	1.9 ± 0.34	0.8 ± 0.19	6.9×10^{-3}
Insulitis (range 0–3)	2.6 ± 0.14	0.9 ± 0.25	0.2×10^{-3}
Islet mass (range 0–1)	0.3 ± 0.11	0.8 ± 0.09	1.3×10^{-3}
β-Cell granulation (range 0–100)	31.1 ± 12.2	92.7 ± 4.25	0.2×10^{-4}
Total score (mass × granulation)	13.0 ± 7.08	72.5 ± 9.42	0.2×10^{-3}

Data are means ± SE.